MEDWIN PUBLISHERS
Committed to Create Value for Researchers

International Journal of Biochemistry & Physiology
ISSN: 2577-4360

Isolation and Characterization of Submitochondrial Reticulum Complex Associated with Midpiece of Bovine Cauda Epididymal Sperm

Nagdas SK*, Sharpe B and Tabor M

Department of Chemistry, Physics & Materials Science, Fayetteville State University, USA

***Corresponding author:** Subir K Nagdas, Department of Chemistry, Physics, & Materials Science, Fayetteville State University, 1200 Murchison Road, Fayetteville, USA, Tel: 910-672-2073; Email: snagdas@uncfsu.edu

Research Article

Volume 9 Issue 2

Received Date: July 10, 2024

Published Date: July 24, 2024

DOI: 10.23880/ijbp-16000253

Abstract

The mitochondrial sheath of mammalian spermatozoa adheres to an underlying organized network of electron-dense material termed the submitochondrial reticulum (SMR). The objective of the present study is to characterize the structural components of the SMR. We have isolated SMR fractions from midpieces of bovine cauda sperm. SDS-PAGE of SMR fractions revealed four major polypeptides of 56kDa, 54kDa, 34kDa, and 31kDa. Proteomic analyses of the four polypeptides revealed that 56kDa and 54kDa polypeptides identified as glycerol kinase and 34kDa and 31kDa polypeptide identified as VDAC2 and VDAC3, respectively (Voltage-Dependent Anion-Selective Channel Protein 2/3). Western blots of midpiece stained with anti-56kDa, anti-54KDa, anti-34kDaVDAC2, and anti-31kDaVDAC3 antibodies demonstrated the presence of 56kDa, 54kDa, 34kDa, and 31kDa immunoreactive bands, respectively. Four polypeptides are localized to midpiece. Glycerol kinase activity was quantitively assayed in tails. We proposed that glycerol kinase and VDAC2/VDAC 3 polypeptides play an important role in sperm motility and in midpiece function.

Keywords: Epididymis; Sperm; Sperm Midpiece; Sperm Motility; Glycerol Kinase; VDAC2; VDAC3

Abbreviations

SMR: Submitochondrial Reticulum; ODF: Outer Dense Fibers; TNI: Tris-Saline-Protease Inhibitor Solution; MP: Midpieces; NCBI: National Center for Biotechnology Information; BSA: Bovine Serum Albumin; VDAC: Voltage Dependent Anion Selective Channels.

Introduction

A hallmark feature of the mammalian spermatozoa is the highly polarized architecture of its individually segregated organelles [1]. The spermatozoa consist of two major structures, the head and tail. The "neck" is the location where the head and tail are connected. The tail is divided into three segments: midpiece, principal piece, and end piece. The mitochondria of the mammalian spermatozoa are localized in the tail, more specifically, the midpiece segment of the tail where they wrap in a helical fashion around the structural elements of the flagellum [2]. Mitochondria are sites of oxidative phosphorylation and cellular energy production [2]. Mitochondria are highly dynamic and motile; change in shape and size and undergo fusion, fission, transport, and mitophagy [3-5]. Male infertility could be due to

mitochondrial disorder, for example, hypospermatogenesis and asthenozoospermia [6].

The core of the midpiece is the flagellar cytoskeleton that is composed of microtubule-based exoneme and the nine outer dense fibers (ODF). Each mitochondrion has three distinct surfaces that include the plasma membrane, neighboring mitochondria, and the outer dense-fiber-axoneme complex [1]. A poorly identified network of cytoskeletal filaments called submitochondrial reticulum (SMR) complex lies between the ODFs and the mitochondria which are associated with the outer mitochondrial membrane [1,7]. By thin-section electron microscopy, Olson and Winfrey [1,7] identified this SMR complex, localized within the midpiece, consisting of inter-connected ribbons of electron-dense material. The SMR is a cylinder-shaped lattice of electron-dense material, associated with the inner surface of the mitochondrial sheath [1]. The SMR ends distally at the midpiece-principal piece junction where it fuses with the annulus. This submitochondrial reticulum complex may be involved in mitochondrial migration to the midpiece during spermiogenesis and/or provide a framework which selectively restrains mitochondria at this intracellular site. Both biochemical analyses and structural examinations are required to define its function. The objective of the present study is to identify and to characterize the structural components of the SMR and to examine the biochemical properties of the SMR complex.

Materials and Methods

Animals

Care and use of animals conformed to NIH guidelines for humane animal care and use in research and all protocols were approved by the Institutional Animal Care and Use Committee of Benedict College (Columbia, SC). Animals were maintained in Benedict College animal care facility with free access to food and water and under the care of veterinarian of Benedict College.

Sperm Preparation and Isolation of SMR Complex

Bovine epididymides were purchased from Randloph Packing, Asheboro, North Carolina. Epididymides were stored at 4^0C during transit and utilized for sperm preparation within 30 minutes of retrieval. Cauda epididymal regions were removed from the organ, minced, and incubated for 5 minutes at 37^0C in Hank's balanced saline solution, pH 7.4, containing 5mM HEPES, 2 mM benzamidine, and 0.05% sodium azide. To evaluate cellular viability, sperm were examined by phase-contrast microscopy. Sperm suspensions were centrifuged at 100 x g for 1 minute to sediment epididymal tubule fragments. Supernatants were centrifuged at 1500 x g for 10 minutes at 4^0C using an Eppendorf Centrifuge. Pellets were washed 3 times by resuspension in Hanks balanced saline solution, as stated above, following which they were resuspended in a Tris-saline-protease inhibitor solution (TNI) containing 150 mM NaCl, 25 mM Tris-HCl, (pH 7.5), 2 mM benzamidine, 1 µg/mL leupeptin, 1 µg/mL pepstatin, and 0.05% sodium azide and centrifuged at 1500 x g for 10 minutes at 4^0C. Resulting pellets were washed 2 more times in TNI as stated above. Bovine Cauda Sperm were sonicated and the midpieces (MP) were isolated by discontinuous sucrose density gradient centrifugation, following the method of Nagdas SK, et al. [8]. Submitochondrial Reticulum Complex (SMR) fractions were isolated from MP extracting MP in DTT (2mg/mL) and 0.2% Triton X-100. Subsequently, the pellet after extraction was subjected to discontinuous sucrose-density gradient (30%, 50%, and 60%) centrifugation. The SMR band was collected at the 50/60 interface. Purified sperm tails and heads were isolated from sonicated sperm by centrifugation on sucrose density gradients centrifugation as described previously [8].

Glycerol Kinase Assay

Glycerol Kinase activity was assayed spectrophotometrically following the method of Worthington Enzyme Manual [9]. One-unit results in the oxidation of one micromole of NADH per minute at 25^0C. Proteins were estimated by the method of Bradford [10]. Glycerol kinase sensitivity to AMP was examined at a different concentration of AMP (0.1-0.9 mM) in the assay buffer.

Antibody Preparation of SMR 56 and SMR 54 polypeptides: For antibody preparation, the SMR fraction was subjected to final purification by preparative SDS-PAGE. After staining with $CuCl_2$ [11], SMR56 and SMR54 bands were excised and used for immunization of rabbits. SMR 56 and SMR54 gel slices were homogenized separately with Freund's complete adjuvant for the primary injection and with Freund's incomplete adjuvant for two booster injections given at 2-wk intervals. Blood was collected by anesthetized animals by cardiac puncture. An IgG fraction, purified by protein A Sepharose affinity chromatography was used for immunoblotting or immunocytochemistry [12].

SDS-PAGE, Western Blotting, and Immunocytochemistry

SDS-PAGE was performed on 12% polyacrylamide gels [13]. Polypeptide bands were stained with Coomassie blue [14]. Proteomic identification of four major polypeptides by MALDI-TOF-TOF analysis to obtain internal amino acid sequences of several tryptic peptides, were performed at the Mass Spectrometry Facility of UNC School of Medicine

Proteomic Center, Chapel Hill, NC. Derived peptide sequences were analyzed in the National Center for Biotechnology Information (NCBI) database for the determination of potential functional motifs, including a transmembrane hydrophobic domain, an extracellular domain with consensus glycosylation sites, and to define potential phosphorylation sites and protein interaction domains on its cytoplasmic segment.

Western Blot analysis was performed by the electrophoretic transfer of polypeptides to PVDF membranes [15]. Immunoblots were briefly rinsed with TBS buffer containing 10mM Tris-HCl pH 7.5, 100 mM NaCl and 0.1% Tween-20 (TBS-0.1% Tween-20) prior to blocking. To prevent non-specific binding, membranes were blocked in a solution containing TBS-0.1% Tween-20 and 1% Bovine Serum Albumin (BSA) for 1 hour at room temperature. Blots were incubated with primary antibodies (1:2000 dilution) in blocking solution for 1 hour at room temperature. Membranes were washed three times (3 minutes per wash) with TBS-0.1% Tween-20 and incubated with IRDye ® 680RD, goat anti-rabbit for LICOR Odyssey CLx Imaging System or an affinity purified horseradish peroxidase-conjugated secondary antibody (1:5000 dilution) for color reaction. Immunoreactive protein bands were identified using LICOR Odyssey CLx Imaging System or by color development using H_2O_2 and diaminobenzidine.

For immunofluorescence microscopy, cauda epididymal sperm were fixed at 4oC in 4% formaldehyde in 0.1 M sodium phosphate buffer, pH7.6, for at least 30 minutes, attached to poly-L-Lysine coated coverslips, washed with PBS, and permeabilized by incubation for 10 minutes in -20^{0}C acetone. After three rinses in PBS, nonspecific protein binding sites were blocked in PBS containing 0.1% Tween-20 and 2.5% BSA (blocking solution). Coverslips were then incubated with primary antibodies (1:2000 dilution) in blocking solution for 1 hour at room temperature, washed and incubated with Cy3 or FITC-conjugated goat anti-rabbit IgG (KPL Inc., Gaithersburg, MD) in blocking solution. Coverslips were washed with PBS and the cells were examined by phase contrast and epifluorescence microscopy.

Results and Discussion

Polypeptide Composition of SMR Fraction and Proteomic Identification

In the present, we have isolated SMR fractions from midpieces of bovine cauda sperm. SDS-PAGE of SMR fractions revealed four major polypeptides of 56kDa, 54kDa, 34kDa, and 31kDa (Figure 1). Proteomic analyses of 56kDa, and 54kDa by MALDI-TOF-TOF yielded 33 and 21 peptides, respectively (Table 1) that matched the NCBI data sequences of glycerol kinase. MALDI-TOF-TOF analyses of 34kDa, and 31kDa polypeptides yielded 24 and 34 peptides, respectively (Table 2). The NCBI data sequences matched 34kDa and 31kDa polypeptide identified as VDAC2 and VDAC3, respectively (Voltage-Dependent Anion-Selective Channel Protein 2/3).

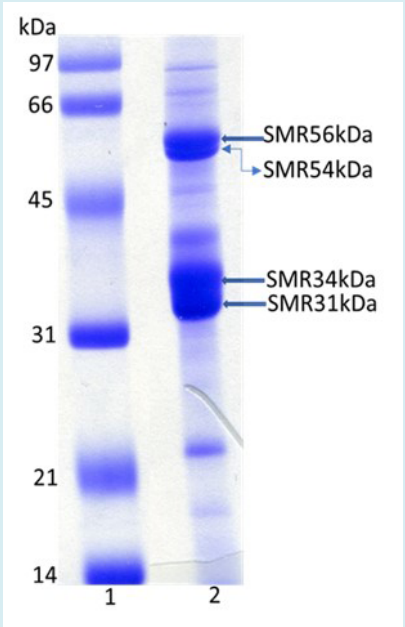

Figure 1: Coomassie blue-stained SDS-PAGE of isolated SMR fractions (15µg) under reducing conditions (lane 2). Lane 1 represents molecular weight standard proteins.

SMR 56kDa	SMR 54kDa
K) KAVLGPLVGAVDQGTSSTR	(K) KAVLGPLVGAVDQGTSSTR
(K) KAVLGPLVGAVDQGTSSTR	(K) AVLGPLVGAVDQGTSSTR
(K)LAKEVGTSYGCYFVPAFSGLYAPYWEPSAR	(R) GIICGLTQFTNK
(K)AVLGPLVGAVDQGTSSTR	(K) LGQLNIDISNIK
(K) LGQLNIDISNIK	(R) SSSEIYGLM*K
(R) GIICGLTOFTNK	(R) EILDAM*NR
(K) TAELLSHHQVEIK	(R) SSSEIYGLMK
(K) SKTGLPLSTYFSAVK	(R) EILDAMNR
(R) SSSEIYGLMK	(R) DNLGIIK
(K) AVLGPLVGAVDQGTSSTR	(R) WLLDNVR
(R) WLRDNLGIIK	(R) TQSTVESLSK
(K) TGLPLSTYFSAVK	(R) IPGNNNFVK
(R) TQSTVESLSK	(R) FLVFNSK
(R) EILDAMNR	(R) TM*LFNIHSLEWDK
(R) WLLDNVR	(R) ETTVVWDK
(K) LGOLNIDISNIK	(R) WLLDNVRK
(R) DNLGIIK	(R) ETTVVWDK
(K) AIGVSNQR	(R) DNLGIIK
(K) TGLPLSTYFSAVK	(R) WLLDNVR
(R) EGWVEQDPK	(R) EILDAMNR
(R) WLRDNLGIIK	(K) TGLPLSTYFSAVK
(R) FLVFNSK	
(R) EILDAM*NR	
(R) ETTVVWDK	
(K) AIGVSNQR	
(R) SSSEIYGLMK	
(R) TMLFNIHSLEWDK	
(R) FLVFNSK	
(R) DNLGIIK	
(R) TQSTVESLSK	
(R) YSTWKK	
(R) EILDAMNR	
(R) WLLDNVR	

Table 1: Proteomics Analyses of SMR56 and SMR54 Polypeptides by MALDI-TOF-TOF.

SMR 34kDa	SMR 31kDa
(R) TGDFQLHTNVNDGTEFGGSIYQK	(K) AADFQLHTHVNDGTEFGGSIYQK
(R) TGDFQLHTNVNDGTEFGGSIYQK	(K) LAEGLKLTLDTIFVPNTGK
(K) SCSGVEFSTSGSSNTDTGK	(K) SCSGVEFSTSGHAYTDTGK
(R) TGDFQLHTNVNDGTEFGGSIYQK	(K) VNNASLIGLGYTQTLR
(R) TGDFQLHTNVNDGTEFGGSIYQK	(K) TKSCSGVEFSTSGHAYTDTGK
(K) WNTDNTLGTEIAIEDQICQGLK	(K) AADFQLHTHVNDGTEFGGSIYQK
(K) YKWCEYGLTFTEK	(K) SKLSONNFALGYK
(R) DIFNKGFGFGLVK	(R) IETSINLAWTAGSNNTR
(K) LTFDTTFSPNTGKK	(K) VNNASLIGLGYTQTLRPGVK
(K) VNNSSLIGVGYTQTLRPGVK	(K) LAEGLKLTLDTIFVPNTGKK
(K) LTLSALVDGK	(K) VNNASLIGLGYTQTLRPGVK
(K) SCSGVEFSTSGSSNTDTGKVTGTLETK	(K) LTLSALIDGKNFNAGGHK
(K) WCEYGLTFTEK	(K) DVFNKGYGFGM*VK
(K) VNNSSLIGVGYTQTLRPGVK	(K) VNNASLIGLGYTQTLRRGVK
(K)VNNSSLIGVGYTQTLRPGVKLTLSALVDGK	(K) LAEGLKLTLDTIFVPNTGK
(R) NNFAVGYR	(K) DVFNKGYGFGMVK
(K) LTFDTTFSPNTGKK	(K) LSQNNFALGYK
(K) VTGTLETK	(K) LTLSALIDGK
(R) NNFAVGYR	(K) LSQNNFALGYK
(K) YQLDPTASISAK	(K) LTLDTIFVPNTGK
(K) LTLSALVDGK	(K) LTLDTIFVPNTGK
(K) GFGFGLVK	(K) WNTDNTLGTEISWENKLAEGLK
(K) VTGTLETK	(K) ASGNLETKYK
(K) SINAGGHK	(K) AAKDVFNK
	(K) LTLDTIFVPNTGKK
	(R) IETSINLAWTAGSNNTR
	(K) DVFNKGYGFGM*VK
	(K) GYGFGM*VK
	(K) LTLSALIDGK
	(K) YKLDCR
	(K) NFNAGGHK
	(K) GYGFGMVK
	(K) VGLGFELEA
	(K) GYGFGM*VK

Table 2: Proteomics Analyses of SMR34 and SMR31 Polypeptides by MALDI-TOF-TOF.

Biochemical and Immunofluorescence Localization of SMR Polypeptides

Western blot analyses of bovine cauda epididymal spermatozoa tails stained with IgG fraction of polyclonal antibodies of SMR 56kDa and SMR 54kDa polypeptides demonstrated the presence of a immunoreactive SMR56 (Figure 2A, lane 2) and SMR 54 (Figure 2A, lane 3) bands. Immunoblots of cauda sperm tail lysates stained with anti-VDAC2 and anti-VDAC3 (Abcam, MA, USA) exhibited 34KDa

(VDAC2) (Figure 2B, lane 2) and 31kDa (VDAC3) (Figure 2C, lane 2) bands respectively. No bands were detected when identical blots were stained with nonimmune IgG (data not shown).

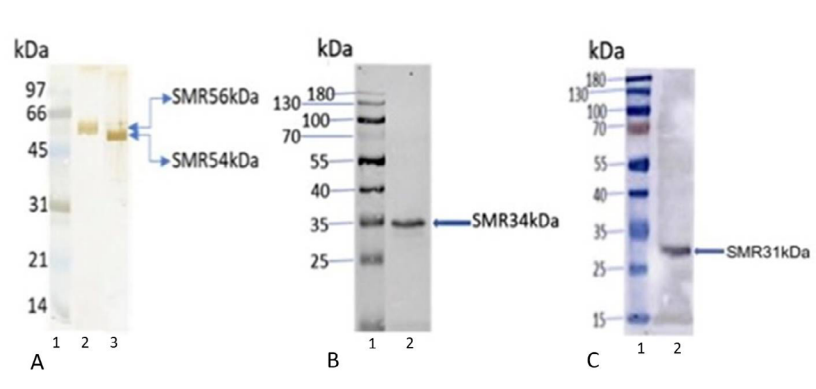

Figure 2: Immunoblot analyses of bovine cauda sperm tails (5µg) stained with anti-SMR 56, anti-SMR54, anti-VDAC2 (SMR 34kDa), and anti-VDAC3 (SMR 31kDa) antibodies revealed the presence of 56kDa (A-lane 2), 54kDa (A-lane 3), 34kDa VDAC2 (B-lane 2), 31kDa VDAC3 (C-lane 2) immunoreactive bands. Lane 1 of figures A, B, and C represents molecular weight standard proteins.

Cauda epididymal spermatozoa stained with IgG fraction of polyclonal antibodies of SMR 56kDa (Figure 3A) and SMR 54kDa (Figure 3B) polypeptides exhibited specific staining of the midpiece. While staining with anti-VDAC2 (Figure 3C) and anti-VDAC3 (Figure 3D), staining was restricted to the midpiece. The head and principal piece displayed no detectable staining. Sperm stained with nonimmune IgG exhibited no fluorescence (data not shown).

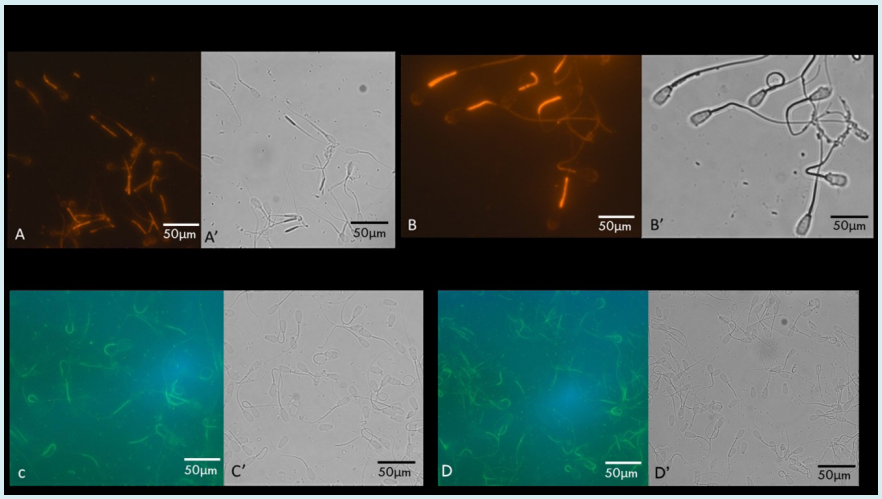

Figure 3: Immunocytochemical localization of four SMR polypeptides-Fluorescence and phase-contrast images of bovine cauda sperm immunostained with anti-SMR56 (A and A'), anti-SMR54 (B and B'), anti-34kDa VDAC2 (C and C'), and anti-31kDa VDAC3 (D and D') antibodies exhibited intense staining of the midpiece segment of the tail. Bar=50 µm.

Biochemical Fractionation of SMR Polypeptides

To identify the association of SMR polypeptides with specific particulate sperm structures, a sequential extraction strategy was used. Western blots of total tails lysate (lane 1 of Figure 4A-C), the Triton X-100-soluble tails fraction (lane 2 of Figure 4A-C), the Triton X-100-DTT soluble tails fraction (lane 3 of Figure 4A-C), the soluble fraction after RIPA buffer (1% Triton X-100, 1% sodium deoxycholate, 0.1% SDS, 0.15 M NaCl, proteases inhibitors in 10 mM sodium phosphate buffer, pH 7.2) extraction (lane 4 of Figure 4A-C), and the tails pellet obtained after RIPA buffer extraction (lane 5 of Figure 4A-C) stained with IgG fraction of polyclonal antibodies of SMR 56kDa (Figure 4A), SMR

54kDa (Figure 4B) polypeptides, and anti-VDAC3 (Figure 4C) exhibited the presence of SMR 56kDa, SMR 54kDa, and SMR 31kDa polypeptides in the total sperm lysate (lane 1 of Figure 4A-C) and in the supernatant fraction obtained after RIPA buffer extraction (lane 4 of Figure 4A-C). No band was seen when identical blots were stained with nonimmune IgG (data not shown). These experiments demonstrate that SMR polypeptides are the structural components of midpiece of flagellum of bovine cauda epididymal spermatozoa.

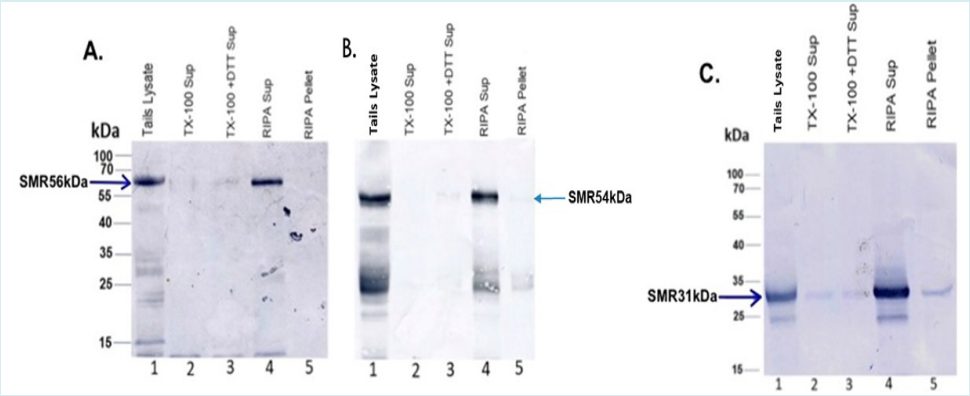

Figure 4: Solubility properties of SMR polypeptides were examined via sequential extraction tails (lane 1 of figures A, B, and C), the Triton X-100-soluble tails fraction (lane 2 of figures A, B, and C), the Triton X-100-DTT soluble tails fraction (lane 3 of figures A, B, and C), the soluble fraction after RIPA buffer extraction (lane 4 of figures A, B, and C), and RIPA buffer extracted tails pellet (lane 5 of figures A, B, and C) immunostained with anti-SMR56 (Figure A), anti-SMR54 (Figure B), and anti-31kDa VDAC3 (Figure C) antibodies. Our results revealed that all SMR polypeptides (56kDa, 54kDa, and 31kDa) were released by RIPA buffer extraction.

Distribution of Glycerol Kinase in Bovine Cauda Sperm Heads and Tails

Our proteomic analyses identified that SMR 56kDa and SMR 54 polypeptides are glycerol kinase. Next, we assayed glycerol kinase activity spectrophotometrically in total sperm lysate and determined the quantitative distribution of glycerol kinase in isolated heads and tails. Glycerol kinase activity was present in total sperm lysate (Figure 5), Major fraction of glycerol kinase activity (approximately 86%) was present in the tails while the remainder was present in the heads (Figure 5). These experiments biochemically confirm that SMR polypeptides are the structural components of the tails, particularly in the midpiece segment of tails.

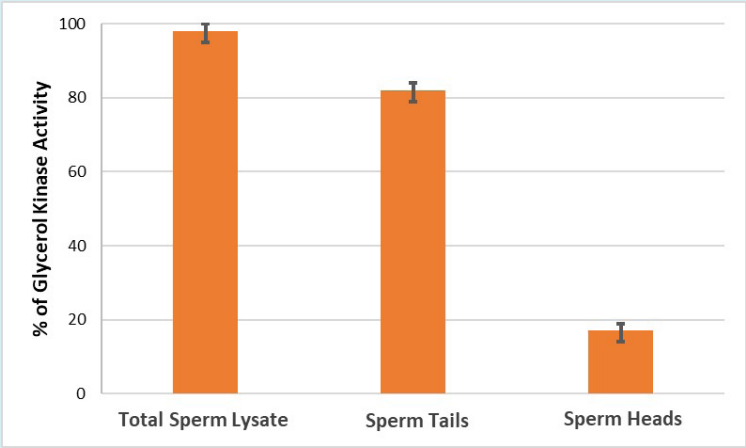

Figure 5: Biochemical assay of glycerol kinase in bovine cauda sperm tails and heads was performed. A major fraction of glycerol kinase activity was present in the tails (~86%), whereas the remainder (~14%) was present in the heads. Enzyme activity of glycerol kinase in total sperm lysate is 10.7 units per mg protein at 25^{0}C. Values represent mean ± SD of three experiments.

Kinetic Properties of Glycerol Kinase

The kinetic properties of glycerol kinase of bovine sperm midpiece fraction were examined spectrophotometrically. The apparent Michaelis-Menten constant (Km) of glycerol kinase for the substrate glycerol was 0.01mM (Figure 6). AMP inhibited glycerol kinase activity (Figure 7) in a dose-dependent manner; 0.4mM AMP exhibited a 50% Inhibition of glycerol kinase activity. Our future studies will address the type of inhibition illustrated by AMP and examine the effect of AMP in sperm motility.

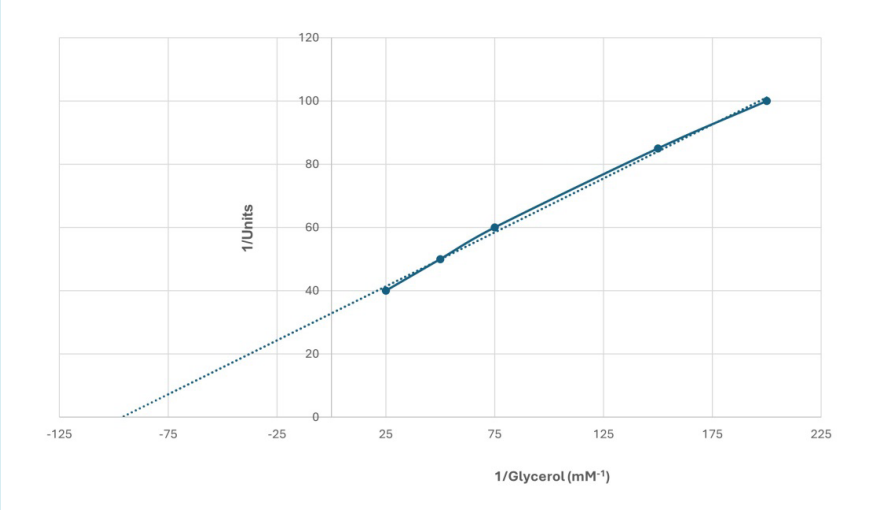

Figure 6: Double reciprocal plot for Glycerol as a substrate (25 to 200 mM) on the activity of glycerol kinase in bovine cauda sperm tails. Sperm tails were extracted in RIPA buffer for two hours at 4^0C, centrifuged at 40000 rpm for 30 minutes at 4^0C in a Beckman TL-55 rotor, and the supernatant obtained after RIPA buffer extraction was dialyzed against 25mM Tris-HCl buffer, pH 7.5 overnight at 4^0C. Glycerol kinase activity of the dialyzed supernatant was assayed at different concentrations of glycerol. One-unit results in the oxidation of one micromole of NADH per minute at 25^0C. The results are representative of three experiments.

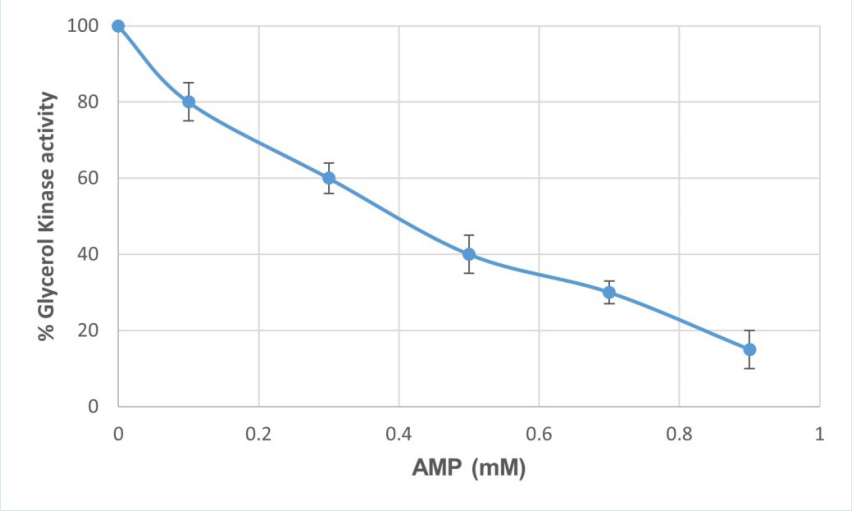

Figure 7: Dose dependent inhibition of glycerol kinase activity by AMP (0.1 to 0.9 mM). Sperm tails were extracted in RIPA buffer for two hours at 4^0C, centrifuged at 40000 rpm for 30 minutes at 4°C in a Beckman TL-55 rotor, and the supernatant obtained after RIPA buffer extraction was dialyzed against 25mM Tris-HCl buffer, pH 7.5 overnight at 4°C. Different concentrations of AMP were incubated with dialyzed supernatant of RIPA buffer extracted bovine sperm tails for 15 minutes, prior to enzyme assay. The data are shown as a percent of glycerol kinase activity of the control. Values represent mean ± SD of three experiments.

Glycerol kinase converts glycerol to glycerol-3-phosphate, a substrate for glycolysis and lipid biosynthesis [16-18]. Testis-specific glycerol kinase-like genes reported in several species and localized [6]. In addition, Chen Y, et al. [6] also showed that GK2 knock-out mice are infertile and GK2 null mice have short mitochondrial sheath and fragmentation of mitochondria. Shimada K, et al. [19] reported that in mice GK2 is needed for the correct organization of crescent-like mitochondria in the formation of mitochondrial sheath during spermiogenesis. Disrupting sperm-specific isoforms of glycerol kinase leads to gaps in the mitochondrial sheath [6,19]. Leung MR, et al. [20] showed that mitochondria are joined to their neighbors via inter-mitochondrial linkers and underlying cytoskeleton through conserved protein arrays on the outer mitochondrial membrane and the protein arrays consist of GK-like proteins. Our results reveal that 56kDa and 54kDa polypeptides in bovine SMR fractions are glycerol kinase and both are localized in flagella. Solubilization experiments illustrate that both 56kDa and 54kDa polypeptides are structural components. Ultrastructural localization will elucidate the discrete localization of 56/54kDa glycerol kinase. In addition, future studies will address identifying specific protein-protein interaction between the SMR and outer mitochondrial sheath in examining the molecular structures of mitochondrial configurations in mammalian sperm.

VDAC (voltage-dependent anion-selective channels) proteins have been studied extensively n somatic cells [21], the role of VDAC in male germ cells is limited. Recently, several studies showed the presence of VDAC in mammalian spermatozoa and participates in spermatogenesis, maturation, and fertilization [22-27]. However, the precise function of VDAC in mammalian spermatozoa remains unclear. Mitochondrial porins of VADCs are transmembrane pore-forming proteins [22]. VDAC2 and 3 are present in the outer dense fiber (ODF) of bovine sperm tails [23]. VDAC2 and VDAC3 in bovine ODF may be involved in trafficking and channeling of ATP to the distal dynein ATPases in the principal piece and/or in protecting ATP from premature hydrolysis [23]. In addition, Hinsch KD, et al. [23] suggested that both VDAC2 and VDAC3 in ODF are involved in the regulation of sperm motility. It has been shown that VDAC2 isoform is an important component of the cell death pathway [28]. VDAC3-deficient males are infertile because of structural abnormalities in the sperm tail, leading to immotile sperm [29]. Several studies showed that VDAC plays important roles in apoptosis, metabolic transport between mitochondria and cytosol, energy metabolism, and cell volume regulation in somatic cells [30]. VDAC present in plasma membrane act as anion channels involved in the regulation of cell volume [24,31]. Mouse VDAC protein undergoes tyrosine phosphorylation during capacitation [32]. Liu B, et al. [33] showed that VDAC were synthesized and secretes in the testis and were finally expressed in the flagella of mature human spermatozoa. It has been reported in several studies that the interaction between VDAC proteins and cytoskeletal proteins may be involved in the integrity of flagellar cytoskeleton [29]. High expression of VDAC2 mRNA has a positive correlation with low sperm motility in male infertility with idiopathic asthenozoospermia [34]. In human spermatozoa, VDAC is present in the tails and involved in the sperm acrosome reaction through mediation of calcium transmembrane transport [26,35]. Incubation of human sperm with anti-VDAC antibody reduces sperm motility through inhibition of calcium transmembrane flow suggesting that VDAC participates in the modulation of human sperm motility [21]. It has been shown by Pan L, et al. [36] that VDAC3 genetic variants may be associated with human sperm count. In mice, Shimada K, et al. [37] identified armadillo repeat-containing 12 (ARMC12) is an essential protein for mitochondrial sheath formation. They proposed that ARMC12 uses VDAC2 and VDAC3 as scaffolds to link mitochondria indicating ARMC12 plays an important role in the formation of mitochondrial sheath through cooperative interactions with several proteins on the sperm mitochondrial surface. Recently, Mise S, et al. [38] identified two sperm specific polypeptides, Kastor and Polluks, previously identified as noncoding RNAs. Both Kastor and Polluks interact with VDAC3 and play an important role in VDAC3-dependent mitochondrial sheath formation needed for male fertility.

Our results reveal that 34kDa and 31kDa polypeptides in bovine SMR fractions are VDAC2 and VDAC3 and both are localized in sperm tails. Ultrastructural localization studies will elucidate the discrete localization of VDAC2 and VDAC3. In addition, our future studies will address identifying VDAC2 and VDAC3 interacting proteins and elucidate the physiological role of VDAC 2 and VDAC3 co-precipitating proteins in mitochondria formation and in sperm motility. Future studies would be beneficial to investigate the relationship between VDAC and infertility. Potential practical benefits derived from this work will help the cattle industry increase population of cattle and improve the fertilizing capacity of functionally impaired spermatozoa. Future work will clarify the role of glycerol kinase and VDAC 2 & 3 in sperm metabolic pathways that may have a direct effect on the motility of spermatozoa.

Statements & Declarations

Funding: Supported by NSF grant 2153783 (Subir K Nagdas), and NC LSAMP NSF grant (#2010124-FSU Subrecipient PI--Subir K Nagdas)

Competing Interests: The authors have no relevant financial or non-financial interests to disclose.

Author Contributions: Subir Nagdas (Principal Investigator)

conceived the study, analyzed data, and wrote the paper. Beonka Sharpe and Matthew Tabor performed experiments.

Data Availability: The datasets generated during and/or analyzed during the current study are not publicly available due to unpublished results but are available from the corresponding author on reasonable request.

Ethics Approval: Care and use of animals conformed to NIH guidelines for humane animal care and use in research and all protocols were approved by the Institutional Animal Care and Use Committee of Benedict College (Columbia, SC). Animals were maintained in Benedict College animal care facility with free access to food and water and under the care of veterinarian of Benedict College. Animals were sacrificed by CO2 asphyxiation.

Acknowledgement

We are grateful to Dr. Samir S. Raychoudhury, Department of Biology, Benedict College, for the use of animal care facility of Benedict College, Columbia, SC. We thank Ms. Chrystal Cooper-Johnson for technical assistance.

References

1. Olson GE, Winfrey VP (1986) Identification of a cytoskeletal network adherent to the mitochondria of mammalian spermatozoa. J Ultrastruct Mol Struct Res 94(2): 131-139.

2. Baba T, Kashiwagi Y, Arimitsu N, Kogure T, Edo A, et al. (2014) Phosphatidic acid (PA)-preferring phospholipase A1 regulates mitochondrial dynamics. Journal of Biological Chemistry 289(16): 11497-11511.

3. Youle RJ, Van der Bliek AM (2012) Mitochondrial fission, fusion, and stress. Science 337(6098): 1062-1065.

4. Mishra P, Chan DC (2014) Mitochondrial dynamics and inheritance during cell division, development and disease. Nat Rev Mol Cell Biol 15(10): 634-646.

5. Choi SY, Huang P, Jenkins GM, Chan DC, Schiller J, et al. (2006) A common lipid links Mfn-mediated mitochondrial fusion and SNARE-regulated exocytosis. Nat Cell Biol 8: 1255-1262.

6. Chen Y, Liang P, Huang Y, Li M, Zhang X, et al. (2017) Glycerol kinase-like proteins cooperate with Pld6 in regulating sperm mitochondrial sheath formation and male fertility. Cell Discov 3: 17030.

7. Olson GE, Winfrey VP (1990) Mitochondria-cytoskeleton interactions in the sperm midpiece. J. Struct. Biol 103(1): 13-22.

8. Nagdas SK, Winfrey VP, Olson GE (1996) Proacrosin-acrosomal matrix binding interactions in ejaculated bovine spermatozoa. Biol. Reprod 54(1): 111-121.

9. Worthington V (1993) Glycerol Kinase. Worthington Enzyme Manual 209-210.

10. Bradford MM (1976) A rapid and sensitive method for the quantitation of microgram quantities of protein utilizing the principle of protein-dye binding. Analytical Biochemistry 72: 248-254.

11. Lee C, Levin A, Branton D (1987) Copper staining: A five-minute protein stain for sodium dodecyl sulfate-polyacrylamide gels. Anal. Biochem 166(2): 308-312.

12. Harlow E, Lane D (1988) Antibodies: A laboratory manual. Cold Spring Harbor Laboratory.

13. Laemmli UK (1970) Cleavage of structural proteins during the assembly of the head of bacteriophage T4. Nature 227(5259): 680-685.

14. Fairbanks G, Steck TL, Wallach DF (1971) Electrophoretic analysis of the major polypeptides of the human erythrocyte membrane. Biochemistry 10(13): 2606-2617.

15. Towbin H, Staehelin T, Gordon J (1979) Electrophoretic transfer of proteins from polyacrylamide gels to nitrocellulose sheets: Procedure and some applications. Proc Natl Acad Sci USA 76(9): 4350-4354.

16. Sjarif DR, Ploos van Amstel JK, Duran M, Beemer FA, Poll-The BT (2000) Isolated and contiguous glycerol kinase gene disorders: a review. J Inherit Metab Dis 23(6): 529-547.

17. Ohira RH, Dipple KM, Zhang YH, McCabe ER (2005) Human and murine glycerol kinase: influence of exon 18 alternative splicing on function. Biochem Biophys Res Commun 331(1): 239-246.

18. Yeh JI, Kettering R, Saxl R, Bourand A, Darbon E, et al. (2009) Structural characterizations of glycerol kinase: unraveling phosphorylation-induced long-range activation. Biochemistry 48(2): 346-356.

19. Shimada K, Kato H, Miyata H, Ikawa M (2019) Glycerol kinase 2 is essential for proper arrangement of crescent-like mitochondria to form the mitochondrial sheath during mouse spermatogenesis. J Reprod Dev 65(2): 155-162.

20. Leung MR, Zenezini CR, Roelofs MC, Hevler JF, Ravi RT, et al. (2021) In-cell structures of conserved supramolecular protein arrays at the mitochondria-cytoskeleton interface in mammalian sperm. Proc Natl Acad Sci USA

118(45): e2110996118.

21. Liu B, Tang M, Han Z, Li J, Zhang J, et al. (2014) Co-incubation of human spermatozoa with anti-VDAC antibody reduced sperm motility. Cell Physiol Biochem 33(1): 142-150.

22. Guarino F, Specchia V, Zapparoli G, Messina A, Aiello R, et al. (2006) Expression and localization in spermatozoa of the mitochondrial porin isoform 2 in Drosophila melanogaster. Biochem Biophys Res Commun 346(3): 665-670.

23. Hinsch KD, De Pinto V, Aires VA, Schneider X, Messina A, et al. (2004) Voltage-dependent anion-selective channels VDAC2 and VDAC3 are abundant proteins in bovine outer dense fibers, a cytoskeletal component of the sperm flagellum. J Biol Chem 279(15): 15281-15288.

24. Triphan X, Menzel VA, Petrunkina AM, Cassará MC, Wemheuer W, et al. (2008) Localisation and function of voltage-dependent anion channels (VDAC) in bovine spermatozoa. Pflugers Arch, 455(4): 677-686.

25. Menzel VA, Cassará MC, Benz R, de Pinto V, Messina A, et al. (2009) Molecular and functional characterization of VDAC2 purified from mammal spermatozoa. Biosci Rep 29(6): 351-362.

26. Liu B, Zhang W, Wang Z (2010) Voltage-dependent anion channel in mammalian spermatozoa. Biochem Biophys Res Commun 397(4): 633-636.

27. Kwon WS, Park YJ, El-Mohamed SA, Pang MG (2013) Voltage-dependent anion channels are a key factor of male fertility. Fertil Steril 99(2): 354-361.

28. Cheng EHY, Sheiko TV, Fisher JK, Craigen WJ, Korsmeyer SJ (2003) VDAC2 inhibits BAK activation and mitochondrial apoptosis. Science 301(5632): 513-517.

29. Sampson MJ, Decker WK, Beaudet AL, Ruitenbeek W, Armstrong D, et al. (2001) Immotile sperm and infertility in mice lacking mitochondrial voltage-dependent anion channel type 3. J Biol Chem 276(42): 39206-39212.

30. Shoshan-Barmatz V, Israelson A, Brdiczka D, Sheu SS (2006) The voltage-dependent anion channel (VDAC): function in intracellular signalling, cell life and cell death. Curr Pharm Des 12(18): 2249-2270.

31. Okada SF, O'Neal WK, Huang P, Nicholas RA, Ostrowski LE, et al. (2004) Voltage-dependent anion channel-1 (VDAC-1) contributes to ATP release and cell volume regulation in murine cells. J Gen Physiol 124(5): 513-526.

32. Arcelay E, Salicioni AM, Wertheimer E, Visconti PE (2008) Identification of proteins undergoing tyrosine phosphorylation during mouse sperm capacitation. Int J Dev Biol 52(5-6): 463-472.

33. Liu, B, Wang Z, Zhang W, Wang X (2009) Expression and localization of voltage-dependent anion channels (VDAC) in human spermatozoa. Biochem Biophys Res Commun 378(3): 366-370.

34. Liu B, Wang P, Wang Z, Jia Y, Niu X, et al. (2010) Analysis and difference of voltage-dependent anion channel mRNA in ejaculated spermatozoa from normozoospermic fertile donors and infertile patients with idiopathic asthenozoospermia. J Assist Reprod Genet 27(12): 719-24.

35. Liu B, Wang P, Wang Z, Zhang W (2011) The use of anti-VDAC2 antibody for the combined assessment of human sperm acrosome integrity and ionophore A23187-induced acrosome reaction. PLoS One 6(2): e16985.

36. Pan L, Liu Q, Li J, Wu W, Wang X, et al. (2017) Association of the VDAC3 gene polymorphism with sperm count in Han-Chinese population with idiopathic male infertility. Oncotarget 8(28): 45242-45248.

37. Shimada K, Park S, Miyata H, Yu Z, Morohoshi A, et al. (2021) ARMC12 regulates spatiotemporal mitochondrial dynamics during spermiogenesis and is required for male fertility. Proc Natl Acad Sci USA 118(6): e2018355118.

38. Mise S, Matsumoto A, Shimada K, Hosaka T, Takahashi M, et al. (2022) Kastor and Polluks polypeptides encoded by a single gene locus cooperatively regulate VDAC and spermatogenesis. Nat Commun 13(1): 1071.